NEAR EARTH BODY DETECTION AND LINKING

us the authors us the authors us the authors

The Johns Hopkins University
[1]Dept. of Computer Science, [2]Dept. of Applied Mathematics and Statistics, [3]Applied Physics Laboratory

ABSTRACT

While most asteroid population discovery to-date has been accomplished by earth-based telescopes, it is speculated that most of the smaller Near Earth Objects (NEOs), up to 140 meters in diameter, whose impact can create substantial city-size damage, have not yet been discovered. Further, there are asteroids that cannot be detected with an earth-based telescope given their size or the location of the Sun. Our objective is therefore to develop an efficient asteroid detection and identification algorithm that can be hosted on-board a spacecraft. By having on-board algorithms, the system would also minimize the need to downlink entire images taken by a space-based telescope. We describe one such image processing pipeline we have developed for asteroid detection and also characterize its performance.

Index Terms— Asteroids detection, identification.

1. INTRODUCTION

NASA has a congressional mandate to discover all Near-Earth Objects (NEOs) at least 1 kilometer in diameter. Fortunately, 95% of the NEOs larger than 1 km that have been discovered are likely not to impact Earth. Near-Earth Object search programs [1] are currently almost exclusively accomplished by earth-based telescopes such as MIT's LINEAR [2] project, the NEAT [3] program, the Catalina Sky Survey, or Pan-STARRS [4]. (An exception is JPL's spacecraft-based WISE telescope brought out of hibernation to characterize NEOs in the 3.4 and 4.6 micron infrared bands [5]).

It is notable however that the NEO that has impacted Chelyabinsk, Russia on 15 February 2013 was only about 17 meters in size. The impact of a 50 meter asteroid that caused the Tunguska Event of 1908 could have destroyed an entire city or metropolitan area. It is estimated that only a relatively small fraction of those so called "city-killing" asteroids, particularly objects less than 140 meters in diameter, have been discovered to date. Because of their size, atmospheric effects and the location of the sun, some of these NEOs cannot easily be detected with an earth-based telescope.

Our focus here is therefore on developing an algorithm that can be hosted on-board a spacecraft. Understanding that there are processing and resources (memory) constraints on-board, our algorithm design needs to not only meet the performance objectives of detecting and identifying asteroids using a space-based telescope, but it also needs to have a small footprint to be implementable with the limited on-board resources. This paper describes an agile algorithm candidate that is being investigated as well as our use of representative space-based imagery for testing it.

There is prior image analysis work for asteroid detection for ground-based image observations. In [4], a reference processing system for detection and identification of asteroid is reported, named the Pan-STARRS Moving Object Processing System (MOPS). This pipeline aims at identifying moving objects in our solar system and linking those detections within and between night observations. It attributes those detections to known objects, calculates initial and differentially corrected orbits for linked detections, recovering detections when they exist, and orbit identification. Most proposed pipelines for earth based detection include a step to combine together images to create a high S/N static-sky image that is subtracted from the current master image to obtain a difference image containing only transient sources. Examples include [6], where a shift-and-add technique is used to improve signal to noise ratio and then synthetically creating long exposure images to facilitate the detection of trajectories. A related shift-and-add method using a median image rather than an average image is reported in [7]. A match filter is used for asteroid detection and matching in [8]. In [9, 10, 11], tree based searches (including KD-trees) are used for efficient linking of successive asteroids detections and finding sets of observation points that can be fitted with an inherent motion model, through an exhaustive search for all possible linkages that satisfy the expected model constraints.

In Section 2 we describe an agile pipeline that can be deployed on an on board system. This approach is both small-footprinted and efficient, and uses Principal Component Analysis rather than tree-based searches to aggregate object detections into trajectories. Since on-board surveys are not available we describe in Section 3 how we validate and test our method using simulated images as well as earth based and space-based image datasets that contain associated ground truth.

This work is supported by NASA Grant XYZ.

2. APPROACH

We describe the main components of our image processing pipeline (shown also in the flow chart in figure 1) addressing detection and linking of asteroids seen in images acquired from space-based platforms. At a high level, the pipeline is summarized as follows: as input to the pipeline is a sequence of time-lapse images. Pre-processing and image registration are used to bring the images into alignment with a common image of reference. Detection of bright bodies is done via thresholding, followed by logical differencing between each image and a reference image containing objects that are common to all registered images in the sequence of images. After differencing, which allows us to detect moving objects, we use an additional step to filter detections based on size and shape considerations (using tools such as connected components and morphological filters). A list of detection coordinates is then generated. Candidate trajectories are then generated for these coordinates by checking rectilinearity (via Principal Component Analysis). A last verification step further checks additional conditions such as the fact that candidate trajectories must be composed of temporally consecutive mover observations. Each module that is detailed next.

Image Pre-Processing We standardize the input images by using a series of photometric and geometric transformations. This includes employing techniques to reduce noise (e.g. median filter) and artifacts that are consequences of the intrinsic properties of the acquisition device. This coordinate information can then be stored in the FITS (Flexible Image Transport System) image header for later use in the Trajectory Verification stage.

Image Registration Image registration refers to finding the transformation that would align multiple images of the same scene that are obtained at different times from slightly different viewpoints. We aim to align each image in the sequence to a common reference image so that the stars in the background line up in all images. In the case of a triplet of images, typically the second image is used as the reference image. We estimate and then apply the necessary translation, rotation, scaling (similarity transformation) and/or skew (full affine transformation) to all images in the sequence such that image objects (stars) are mapped into the same pixels location and so that all transformed images have the same spatial resolution. Image Registration using mutual information [12] and cross-correlation as similarity measures are used.

Image Logical Differencing A global thresholding is applied to the registered image for detecting asteroids and suppressing background noise. As asteroids are typically very faint compared to the surrounding stars, the selection of the detection threshold impacts false alarm rate. Thresholding yields binary detection images. The set of all binary images is then used to generate an intersection image that contains objects that occur in all images in the sequence. This is followed by logical differencing whereby we produce a set of difference images by intersecting the corresponding binary image with the negative of the common intersection image. This operation provides a list of candidate detections for each image in the sequence. While the logical differencing results in good detections, additional artifacts such as crater-like formations are seen as a result of some of the celestial bodies being overexposed. To mitigate this artifact, we subsequently perform filtering out of hollow objects as well as filtering based on object size.

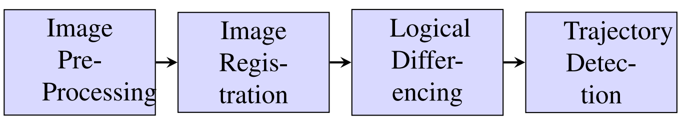

Fig. 1. Image Processing Pipeline

Trajectory Detection The list of centroids of moving objects obtained from image differencing defines a set of candidate rectilinear trajectories. The goal is to find a subset of centroids that fit a linear model. Even though the model is simple, the set of filtered centroids potentially has a high number of noisy points (falsely detected movers), and the cardinality of the set of all candidate trajectories increases exponentially with the number of detections, thus requiring subsequent pruning of this set. We search through all possible trajectories via Principal Component Analysis (PCA) and compute the ratio of eigenvalues, $\lambda_1/(\lambda_1+\lambda_2)$ in order to develop a line confidence score for each candidate trajectory, and choose candidate lines for which this ratio exceeds a threshold. Using the candidate trajectories thus found, we then enforce temporal order of detection by using the sign of the projection on the principal eigenvector. As the final step, we further eliminate false positives by ensuring that the distance between projections is proportional to the time interval between images.

Trajectory Detection(PCA+Tree) - Phil: I added this so that we can talk about this tomorrow. This needs more work. The list of centroids of moving objects obtained from image differencing defines a set of candidate rectilinear trajectories. The goal is to find a subset of centroids that fit a linear model. Even though the model is simple, the set of filtered centroids potentially has a high number of noisy points (falsely detected movers), and the cardinality of the set of all candidate trajectories increases exponentially with the number of detections, thus requiring subsequent pruning of this set. We use a combination of Principal Component Analysis (PCA) and 2d-trees in order to find the trajectories efficiently. Unlike MOPS and CSS(TODO: Add Catalina reference, find the name of their pipeline), we do not set an upper limit on the velocity of the asteroid, and hence do not miss potential fast moving targets. Given a sequence of images, we form all the possible trajectories connecting the detections in the first and last frames. There are $O(n^2)$ trajectories, where n is the number of detections per images. We then find the point of intersection of each of these trajectories with the frames in the middle. We construct a 2 dimensional tree for all the frames in the middle, and perform a range search on the tree to give us the detections that lie within a small radius of the point of intersection. This query can be done on $O(log(n))$ time on average. Once we find a collection of such points that potentially form a linear trajectory, we perform PCA and compute the ratio of eigenvalues, $\lambda_1/(\lambda_1 + \lambda_2)$ in order to develop a line confidence score for each candidate trajectory, and choose lines for which this ratio exceeds a threshold. Using the candidate trajectories thus found, we then enforce temporal order of detection by using the sign of the projection on the principal eigenvector. As the final step, we further eliminate false positives by ensuring that the distance between projections is proportional to the time interval between images. Compared to a brute force line search($O(n^k)$, where k is the number of images in the sequence) our algorithm takes $O(n^2 log(n))$ time. (TODO: Verify this.)

3. EXPERIMENTS

We detail the experiments performed using a range of simulated imagery generated by JHU APL developed Renderer and Camera Emulator (RCE) and real imagery from the NEAT dataset.

3.1. Simulated Imagery

Asteroids are modeled as spherical blackbody-like emitters (emissivity is less than 1), with a cross-sectional area that approximates the sizes of actual asteroids and surface temperatures typical of sun-illuminated asteroids in an Earth-like orbit. Similar to the way stars are modeled, the radiation emitted is modeled using a form of Planck's equation:

$$B_\lambda(T) = \epsilon \frac{2hc^2}{\lambda^5} \frac{1}{e^{\frac{hc}{\lambda k_B T}} - 1} \tag{1}$$

where $B_\lambda(T)$ is the spectral radiance at a given wavelength λ and temperature T (which in SI units would be $Wm^{-2}m^{-1}$). The value ϵ is the emissivity of the asteroid, which essentially converts the blackbody spectral radiance into spectral irradiance. The constant, h is the Planck's constant, c is the speed of light, λ is wavelength, k_B is the Boltzmann constant, and T is the temperature.

The asteroids are assumed to have a nominal temperature of 200 K due to solar heating and emissivities in the range from 0.9 to 0.98. The RCE uses stellar data available as part of the Two Micron All Sky Survey (2MASS), a stellar survey that scanned the entire sky in three IR bands (centered at 1.25 m, 1.65 m, and 2.17 m, respectively). The 2MASS catalog also incorporates data in two visible bands from other surveys. An example of the simulated MWIR image and the ground truth trajectory derived from one set of simulated imagery is shown in Figure 2. Figure 3 shows the final trajectories detected for one triplet and one quadruplet of the simulated MWIR dataset. As is shown in Figure 3, using trajectory verification on a greater number of images in the sequence allows us to quickly disambiguate and reject false trajectories. In this case this trend is readily apparent when going from a triplet to a quadruplet of images.

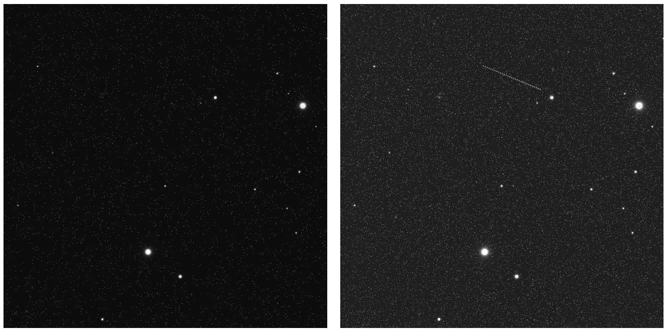

Fig. 2. Left: An image simulated by RCE. Right: 31 simulated MWIR images super-imposed in order to visualize the trajectory of the asteroid in a single image. The true trajectory can be seen as a faint line towards the top center of the image

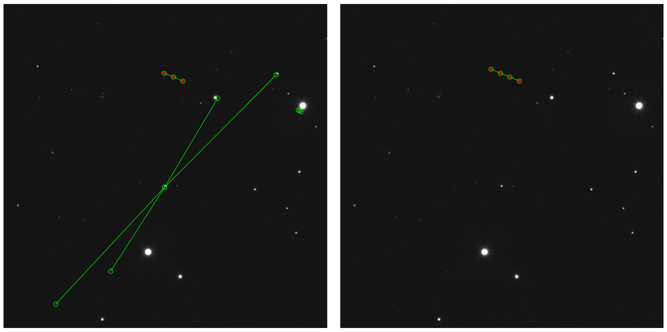

Fig. 3. The trajectories found by the pipeline are shown in green. The true location of the asteroid is marked in red.
Left: Trajectory Detection on a simulated triplet. Right: Trajectory Detection on a quadruplet. Adding one more image to the triplet eliminates the false positives.

3.2. Real Imagery

3.2.1. *NEAT*

Figures 5 and 7 show the results at all stages of the pipeline for one triplet of images of the 2002-CY46 asteroid obtained from the Near Earth Asteroid Tracking (NEAT) [3] survey.

3.2.2. *CATALINA*

3.3. performance characterization

We use the following metrics for algorithm testing and validation. These are used to characterize the performance of the al-

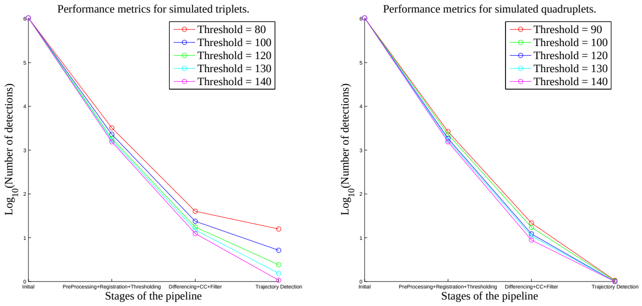

Fig. 4. Left: The number of detections at various stages of the pipeline for triplets of images. Right: The number of detections at various stages of the pipeline for quadruplets of images.

gorithm for the three successive stages: the initial detection of objects, the detection of moving objects and the detection of trajectories: 1. Precision: The fraction of retrieved/detected objects (celestial bodies, moving objects, trajectories) that are relevant, i.e. correspond to correct detections. 2. Recall: The fraction of relevant (true) objects (celestial bodies, moving objects, trajectories) that are actually detected/retrieved. 3. Receiver Operating Characteristic (ROC): A plot of the probability of detection as a function of the probability of false alarm generated by varying a significant parameter of the algorithm (such as the initial detection threshold). This will detail the performance of the system as the parameters of the image processing pipeline are varied. 4. Area under the ROC curve (AUC) that characterizes the performance of detection vs. false alarm with a single metric. 5. Localization error: For those correctly detected asteroids, we will characterize the localization error by computing the 3D (angular pointing error). The simulation and the test image sets have the ground truth location of the asteroid in image coordinates. This true location is compared with the detected trajectory to determine localization error.

The above measures are computed and aggregated over a corpus of images corresponding to a simulated platform and camera.

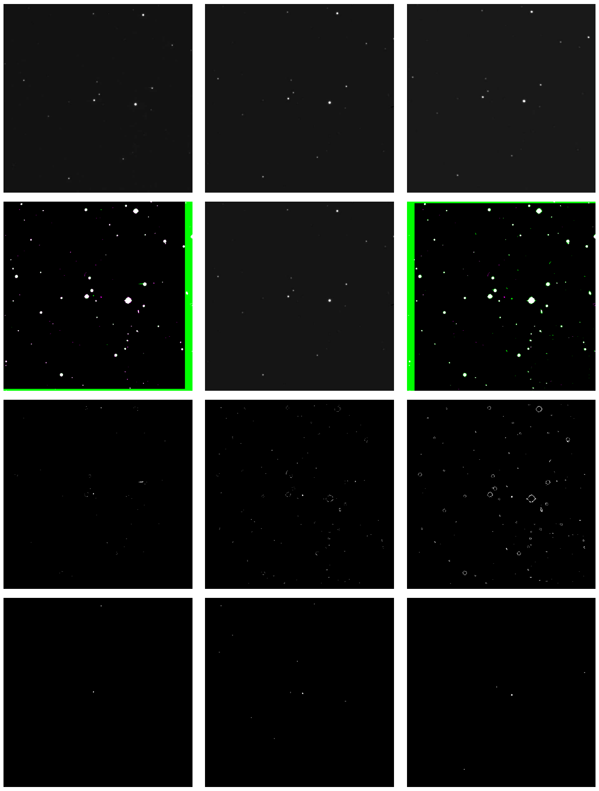

Fig. 5. Image Processing Pipeline results shown on 2002 NEAT data. (row 1): input image triplet (CY46) taken approx. 10 minutes apart. (row 2): Image Registration. Left: Image-1 registered to Image-2. Right: Image-3 registered to Image-2. (row 3): Image Differencing: Artifacts such as crater-like formations are seen in the difference images above. This is the result of some celestial bodies being overexposed.) (row 4): Image Differencing:Filtered centroids shown in each image of the sequence.)

3.4. Footprint characterization

include here some information to the effect that this algorithm is deployable on a reference platform. Efforts are currently being conducted to translate this algorithm in ...

4. CONCLUSION

5. REFERENCES

[1] Grant H Stokes, Jenifer B Evans, and Stephen M Larson, “Near-earth asteroid search programs,” *Asteroids*, vol. 3, pp. 45–54, 2002.

[2] Jenifer B Evans, Frank C Shelly, and Grant H Stokes, “Detection and discovery of near-earth asteroids by the linear program,” *Lincoln Laboratory Journal*, vol. 14, no. 2, pp. 199–215, 2003.

[3] NASA, “The NEAT survey,” 2014.

[4] Larry Denneau, Robert Jedicke, Tommy Grav, Mikael Granvik, Jeremy Kubica, Andrea Milani, Peter Vereš, Richard Wainscoat, Daniel Chang, Francesco Pierfederici, et al., “The pan-starrs moving object processing system,” *Pan*, vol. 125, no. 926, pp. 357–395, 2013.

[5] NASA, “The NEOWISE survey,” 2014.

[6] Michael Shao, Bijan Nemati, Chengxing Zhai, Slava G Turyshev, Jagmit Sandhu, Gregg Hallinan, and Leon K

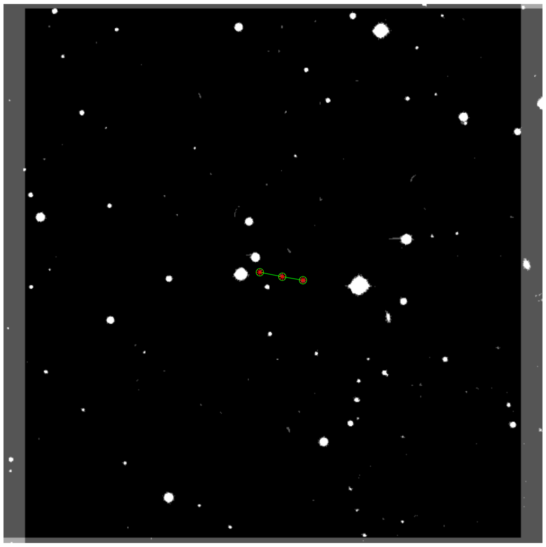

Fig. 7. Trajectory Detection for the NEAT CY46 Triplet. Asteroid trajectory detected is shown in green. True location is in red. 3 Images of the triplet are super-imposed here after registration and thresholding for ease of visualization.

Harding, "Finding very small near-earth asteroids using synthetic tracking," *The Astrophysical Journal*, vol. 782, no. 1, pp. 1, 2014.

[7] Toshifumi Yanagisawa, Atsushi Nakajima, Ken-ichi Kadota, Hirohisa Kurosaki, Tsuko Nakamura, Fumi Yoshida, Budi Dermawan, and Yusuke Sato, "Automatic detection algorithm for small moving objects," *Publications of the Astronomical Society of Japan*, vol. 57, no. 2, pp. 399–408, 2005.

[8] Peter S Gural, Jeffrey A Larsen, and Arianna E Gleason, "Matched filter processing for asteroid detection," *The Astronomical Journal*, vol. 130, no. 4, pp. 1951, 2005.

[9] Jeremy Kubica, Joseph Masiero, Andrew W Moore, Robert Jedicke, and Andrew Connolly, "Variable kd-tree algorithms for spatial pattern search and discovery," *Robotics Institute*, p. 253, 2005.

[10] Jeremy Kubica, Andrew Moore, Andrew Connolly, and Robert Jedicke, "A multiple tree algorithm for the efficient association of asteroid observations," in *Proceedings of the eleventh ACM SIGKDD international conference on Knowledge discovery in data mining*. ACM, 2005, pp. 138–146.

[11] Jeremy Kubica, Larry Denneau, Tommy Grav, James Heasley, Robert Jedicke, Joseph Masiero, Andrea Milani, Andrew Moore, David Tholen, and Richard J Wainscoat, "Efficient intra-and inter-night linking of asteroid detections using kd-trees," *Icarus*, vol. 189, no. 1, pp. 151–168, 2007.

[12] Paul Viola and William M Wells III, "Alignment by maximization of mutual information," *International journal of computer vision*, vol. 24, no. 2, pp. 137–154, 1997.

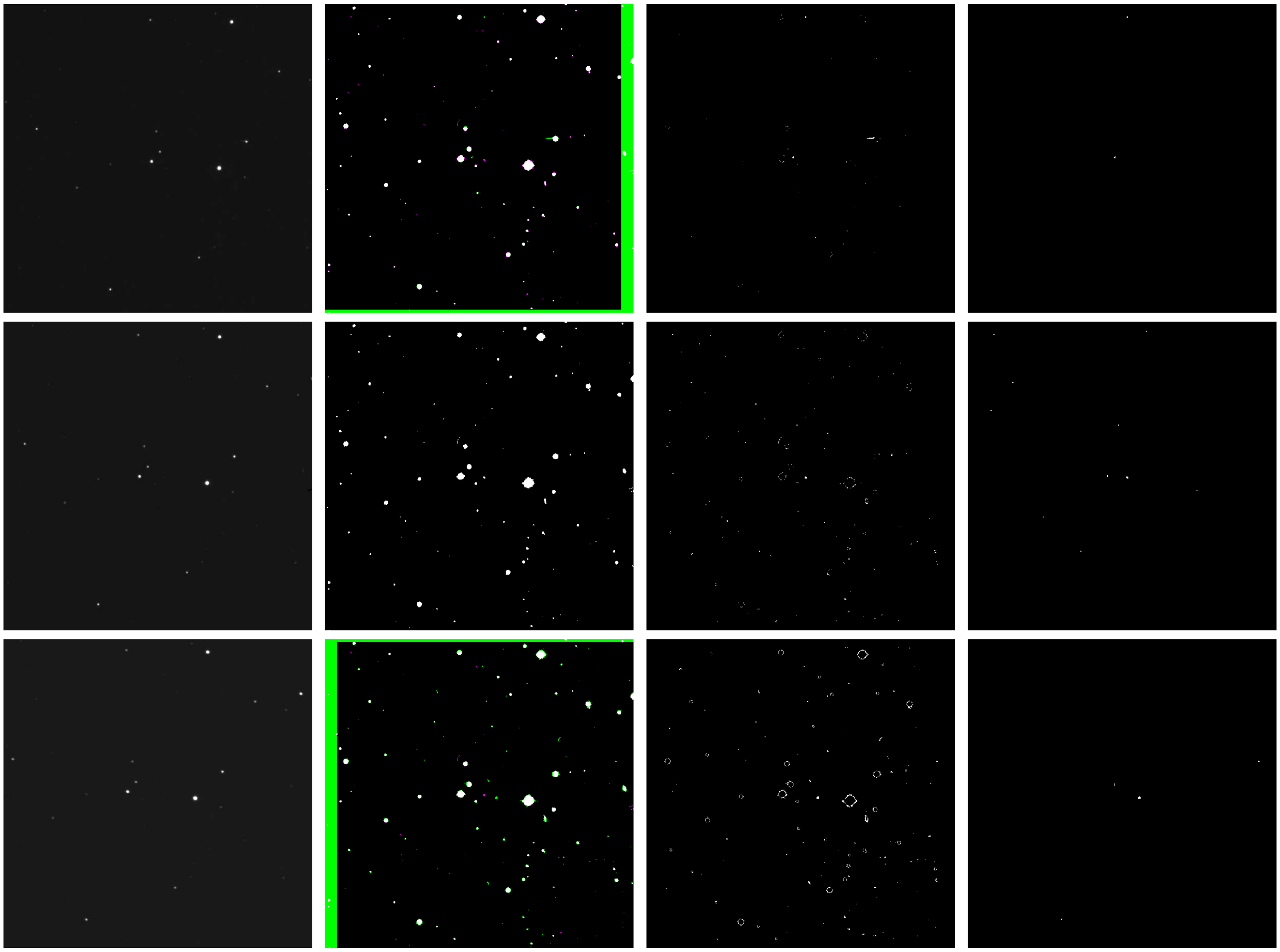

Fig. 6. Image Processing Pipeline results for the CY46 Triplet. First column: 2002 CY46 Triplet images taken approximately 10 minutes apart. Near Earth Asteroid Tracking (NEAT) system archive.

Second column: Image Registration results for the CY46 Triplet. Top: Image-1 registered to Image-2. Middle: Image-2 Bottom: Image-3 registered to Image-2.

Third column: Image Differencing results for the CY46 Triplet. (Artifacts such as crater-like formations are seen in the difference images above. This is the result of some celestial bodies being over-exposed.)

Fourth column: Image Differencing results for the CY46 Triplet. Filtered centroids in each image of the sequence.)